NUMERICAL SIMULATION OF THE SHOCK WAVE INTERACTION WITH A NEAR-WALL FINE PARTICLE LAYER

A.V. Fedorov, N.N. Fedorova, and I.A. Fedorchenko

Institute of Theoretical and Applied Mechanics SD RAS,
630090 Novosibirsk, Russia
Novosibirsk State University of Civil Engineering and Architecture,
630008 Novosibirsk, Russia

Introduction

The dust explosion prevention in mines and dusted industries has been an important issue for years. During this time, many experimental and theoretical investigations have been carried out. Nevertheless, up to now nobody can declare that all the mechanisms are clear and the comprehensive mathematical model is constructed taking into account all the details of this complicated process.

The gas-dust mixture formation behind a shock wave travelling along the dust layer was investigated experimentally by A.A. Borisov et al [1]. In this work, the dust lifting was related to an action of the compression and expansion wave system formed by multiple sequential reflections of the leading shock from rigid wall and contact surface. The simple linear mechanistic model was proposed [2] to explain the experiments that given consistent results. The similar wave picture was obtained in numerical simulations by A.L. Kuhl et al [3, 4] and H. Sakakita [5].

The present paper focuses on numerical simulation of wave processes observed in near-wall fluidized layer under action of normal shock wave. The unsteady process of interaction is described for various shock wave intensities and layer densities. It is shown that shock wave intensity increases significantly in the dense layer, and the gain factor does not depend on the shock wave Mach number and defined only by the density ratio. Two different schemes (regular and Mach) of shock reflections are observed in computations that lead to a principally distinguished scenarios of instability development in a dusty layer.

Problem statement, mathematical model and method of computation

The computation setup is shown in Fig. 1. The planar shock wave, normal to the plate surface, is travelling in still air (u_0=0, ρ_0=1.177 kg/m^3, T_0=288 K) from right to left with a velocity $D = M_s \cdot c_0$ (M_s is the shock wave Mach number and c_0 is a speed of sound before the shock). The u_2, ρ_2 and T_2 values are calculated using the ideal gas-dynamic relations for normal shock. In the moving coordinate system adjusted to the shock, the shock is in rest but the air before the shock has a velocity $-D$, so does the whole plate.

At $x \le 0$ the dense layer of the width h is disposed along the wall. The increased density of the layer $\rho = m_1\rho_0 + m_2\rho_{22}$ is related to the presence of dispersed phase of density ρ_{22} with volume concentration (particle loading ratio) m_2>0 and m_1=1-m_2 is gas volume concentration. The density of the layer can be characterized by the dimensionless value A= $(\rho-\rho_0)/(\rho+\rho_0)$.

In the present study, the gas-dust mixture is assumed to be viscous heat-conductive pseudo-gas described in a frame of one-temperature, one-velocity model of heterogeneous media [6] which is valid for a case of very fine particles. This model includes the conservation laws for the intrinsic mixture parameters that are the non-stationary 2-D Navier-Stokes equations closed by the equation for particle volume concentration m_2

$$\frac{\partial m_2}{\partial t} + \frac{\partial m_2 u}{\partial x} + \frac{\partial m_2 v}{\partial y} = 0$$

Report Documentation Page

Report Date	Report Type	Dates Covered (from... to)
23 Aug 2002	N/A	-

Title and Subtitle Numerical Simulation of the Shock Wave Interaction With A Near-Wall Fine Particle Layer	**Contract Number**
	Grant Number
	Program Element Number
Author(s)	**Project Number**
	Task Number
	Work Unit Number
Performing Organization Name(s) and Address(es) Institute of Theoretical and Applied Mechanics Institutskaya 4/1 Novosibirsk 530090 Russia	**Performing Organization Report Number**
Sponsoring/Monitoring Agency Name(s) and Address(es) EOARD PSC 802 Box 14 FPO 09499-0014	**Sponsor/Monitor's Acronym(s)**
	Sponsor/Monitor's Report Number(s)

Distribution/Availability Statement
Approved for public release, distribution unlimited

Supplementary Notes
See also ADM001433, Conference held International Conference on Methods of Aerophysical Research (11th) Held in Novosibirsk, Russia on 1-7 Jul 2002

Abstract

Subject Terms

Report Classification unclassified	**Classification of this page** unclassified
Classification of Abstract unclassified	**Limitation of Abstract** UU

Number of Pages
6

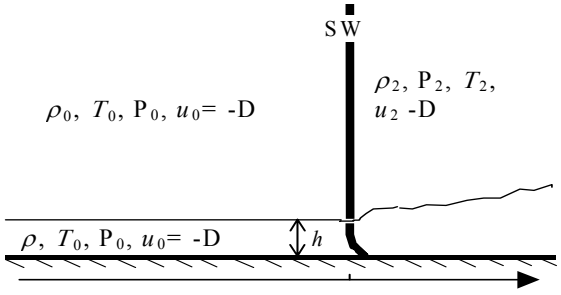

Fig. 1. 2-D problem computation setup in a coordinate system adjusted to shock wave

and the equation of state

$$p = RT\frac{\xi_1\rho}{1-m_2}.$$

Here R stands for the universal gas constant, T and ρ are the mixture temperature and density, ξ_1, ξ_2 are the air and particle specific mass concentrations, consequently, $\xi_i = \frac{\rho_i}{\rho} = \frac{\rho_{ii} m_i}{\rho}$, $\rho_{11}=\rho_0$ and ρ_{22} are the air and particle specific densities. In the present computations the values $\rho_0 = 1.177$ kg/m^3 for air and $\rho_{22} = 1470$ kg/m^3 for coal were used.

For the most of 2-D computations the third-order TVD-upwind method based of Flux Vector Splitting by Van Leer for inviscid terms and the second-order-centered difference scheme for viscous part were used. The description of computation method can be found in [7] where some application of this method for computing the gas-dynamic problems are also provided. For simplified 1-D problem, so-called Cubic Interpolation Propagation (CIP) method [8] was also applied that proved to be useful for problems with strong contact discontinuities.

One-dimensional problem

To clarify the wave picture and to test the method of computation, the problem was at first solved in a simplified 1-D setup. Figure 2 shows the initial conditions (a) and a qualitative flow scheme (b). The impinging shock wave is denoted by SW_1 and the contact surface separated pure and dusted gas is denoted as CS_1. At the moment t_1 SW_1 comes to the contact surface and partially reflects from it as SW_2 and go through to the dense layer as SW_3. Under action of shock wave, contact surface moves toward the wall and the dense layer became thinner. Further, at the moment t_2 the shock reflected from the wall, then comes to the contact surface. As a result of the interaction with the contact surface, the shock partly refracts and goes outside

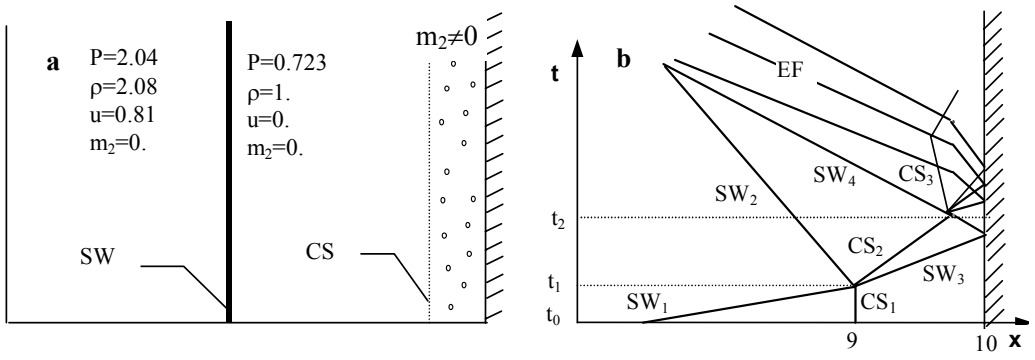

Fig. 2. Test 1-D problem setup (a) and the qualitative flow scheme in the *x*-*t* plane (b)

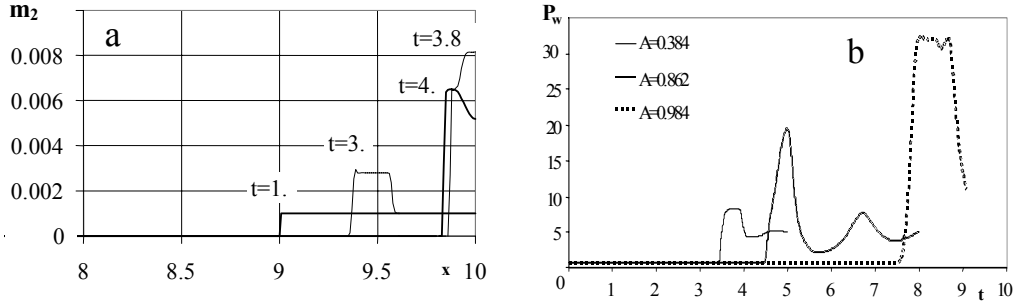

Fig. 3. Distributions of particle volume concentration m_2 at different time moments (a) and pressure distribution along the wall for various initial particle concentrations for M_s=1.6 (b)

the layer as SW_4 and partly reflects as an expansion fan and falls on the wall. After multiple reflections of compression and rarefaction waves from contact surface and rigid wall the wave intensity weakens, pressure distribution becomes constant and the layer is placed near the wall. However, as result action of internal waves, layer thickness may change.

The computation results presented below has been obtained with the help of CIP method, that, together with standard TVD-method, has been used for these computations and demonstrated a good ability in resolving of all the flow peculiarities.

The distributions of particle volume concentration m_2 at different time moments are shown in Fig. 3, a. For this situation at t=0 dust volume concentration is constant at 9<x<10, $m_2=10^{-3}$, that corresponds to A=0.384. At the moment t=1 shock wave still has not come to the contact surface. At t=3 the contact surface are moving toward the wall that causes a significant rise in level of volume concentration in a external part of the layer. Further, at t=3.8 and t=4 the layer is concentrated near wall, and compression and internal expansion waves bring about the changes in m_2 distributions, but, as Fig. 3, a shows, the whole layer remains near the wall and only slight variations in layer thickness can be observed. Figure 3, b demonstrates pressure distribution along the wall for various initial particle concentrations for M_s=1.6. This figure confirms that inside the layer the intensity of the shock wave increases and there are exists a system of the compression and expansion waves.

2-D problem results and discussions

The computations were carried out for h=5 mm, M_s=1.6, 2, 2.5, 3; A=1/5, 1/3, 3/7, 1/2 и 2/3. On the basis of numerical simulations, the wave picture in shock wave vicinity was analyzed.

In Fig. 4, 5 the fields of static pressure and density are shown for M_s = 2, *A=1/3* at t=12 and 36 ms, respectively. At the moment t=0 the shock wave (SW) denoted by *1* reaches the edge of rectangular layer and reflects from it partly by a compression wave (*2*) that propagates from left to right and soon leaves the computational domain. At the same time, the leading shock penetrates into the dense layer. In the moving coordinate system this process is similar to the near-wall dense jet spreading into pure gas. The SW intensity gains in a dense layer and the shock front becomes curved. The oblique shock reflects from wall as a compression wave (*3*) that reaches the contact surface dividing the pure and dusted gas. This contact surface is the edge of near wall dense jet spreading into a pure gas after the SW and can be seen in Fig. 5 (curve *4*). Since the compression wave is going from dense layer into a pure gas, it reflects from contact surface by an expansion fan (*5*) that falls to the wall and reflect from it. Further, the

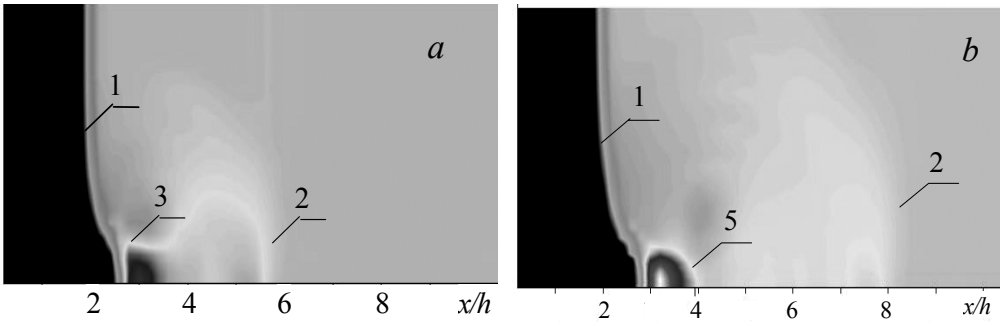

Fig. 4. Static pressure field at t=12 (*a*) and 36 ms (*b*)

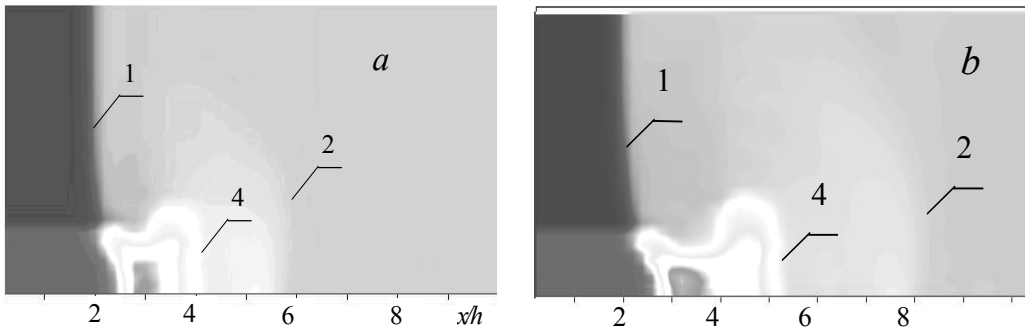

Fig. 5. Density fields at t=12 (*a*) and 36 ms (*b*)

situation repeats, and multiple sequential reflections of compression and expansion wave are formed inside the layer. The intensities of internal waves attenuate with a distance from the leading SW since at every interaction of a wave with the contact surface some part of wave energy is going out of the dense layer and the other is transferred to the reflected wave.

As it was mentioned above, at initial stage of interaction the SW intensity increases and the front of shock wave becomes curved. The gain factor P_{max}/P_2 (a) and the angle between the SW and the plate α are shown in Fig. 6 for various M_s. Figure 6 shows that, with elevation of A, the gain factor increases and α decreases, and they do not depend on M_s.

The oblique SW is reflected from the plate, and depending on M_s and A, both regular and Mach reflection can be realized. Since at low A the SW inclination angle is large, here we have the Mach reflection, and at high A the conditions for regular reflection take place. Figure 7

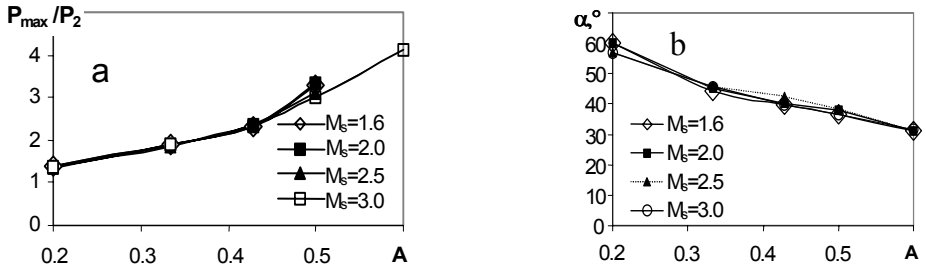

Fig. 6. SW gain factor (a) and angle between SW and plate (b) depending on A for various M_s

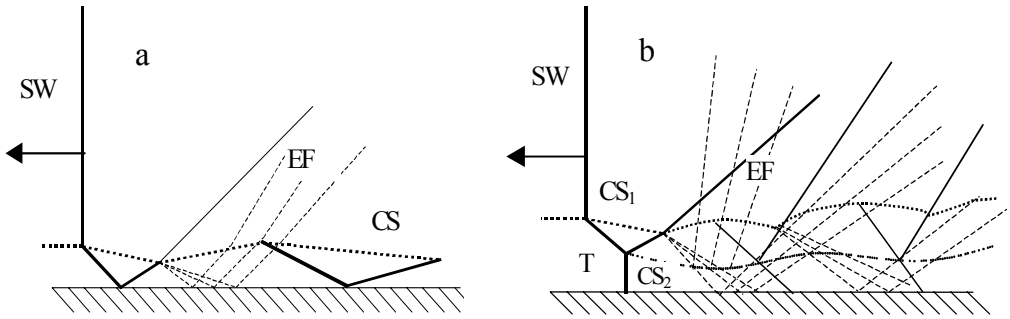

Fig.7. Wave schemes in vicinity of SW interacting with a dense layer for regular (a) and Mach (b) SW reflection

presents the flow schemes for regular (a) and Mach (b) reflections. Here SW denotes the front of leading shock wave, EF is the expansion fan and CS is the contact surface separating pure and dusted gas. At a regular reflection, the wave scheme inside a dense layer is similar to those proposed in [1,2] and was describe above. In this situation the regions of high density are observed on the wall in the places where the compression wave are coming. But for Mach reflection, an additional contact surface CS_2 is originated from a triple-point of λ-configuration formed by incident and reflected SW and Mach stem. The presence of contact surface CS_2 inside the layer changes the wave picture drastically since there is an additional line where internal waves are refracting and reflecting. Downstream from leading SW this contact surface transforms into a jet forming the dense core of the layer. The action of internal wave leads to a formation of spots with high particle concentration inside the layer.

In Fig. 8 the pressure distribution along the wall is shown for M_s=2. Two cases are presented: A=1/3 that corresponds to a typically Mach reflections and A=3/5 where the regular reflection takes place. To compare, the situation without dusty layer (A=0) is also shown. The picture demonstrates the development of the internal waves for these two cases. For Mach reflection (A=1/3) the period of internal wave is shorter and their intensity drops very quickly and after x/h>10 there are no clear evidences of these waves on the pressure plot. For the regular reflection (A=3/5) the internal waves has been observed till x/h=40, but then the regular structures are distracted.

Both for regular and Mach reflection some other disturbances come to the plate after the distraction of internal waves. These disturbances are related to the instability of contact surface divided pure and dusted gas. The development of this instability can be seen in Fig. 9, where density fields are shown for M_s=2, A=1/3. The picture is similar to those observed for near-wall dense jet spreading from left to right. The leading front of the jet rolls up into the vortex-like structure and additional vortices can be seen in the vicinity of the edge of dusted layer. This instability

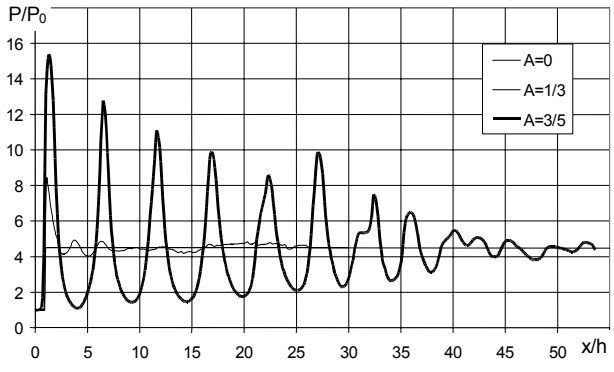

Fig. 8 Pressure distributions at the plate for M_s=2

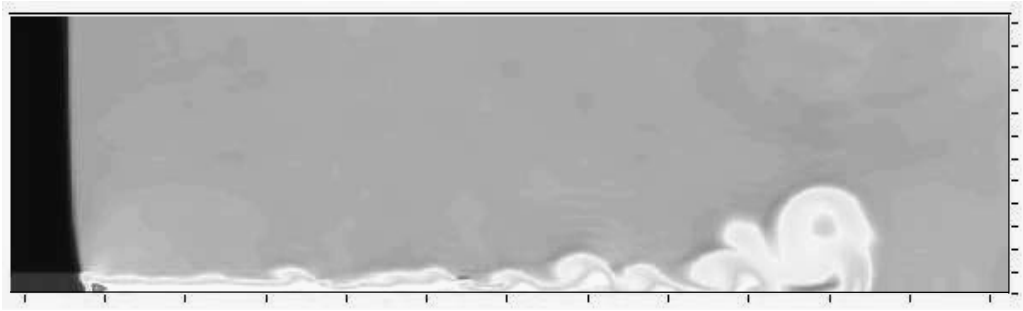

Fig. 9. Density fields at various time moments for M_s=2, A=1/3

leads to a growth of the dusty layer width that can be interpreted as a fine particle lifting under the action of shock wave.

Conclusions

The numerical simulation of the SW interaction with a dusty layer has been carried out in a frame of simplified one-velocity one-temperature mathematical model of heterogeneous media. Two principally different wave pictures in a dense layer were obtained distinguishing by the scenario of shock wave reflection from a rigid wall. For the regular reflection taking place for the high initial layer loading, the wave picture was shown to be similar to those proposed by A.A. Borisov et al. Some peculiarities of internal wave behavior realized in the Mach reflection situation were investigated. A possible reason is proposed to explain the dust lifting from the surface. Namely the growth of the layer width that is a result of the pure-dusted gas interface instability developing at the edge of the dense layer.

Acknowledgements. Work was performed under financial support of ISTC (project 612-B) and Russian Foundation for Basic Research (project 00-01-00891).

REFERENCES

1. **Borisov A.A., Lyubimov A.V., Kogarko S.M. and Kozenko V.P.** On the instability of the bulk material surface under action of glancing shock and detonation waves // Fizika Gorenia i Vzryva, 1967. Vol. 3, No. 1. P. 149-151.
2. **Gelfand B.E., Medvedev S.P., Borisov A.A., Polenov A.N., Frolov S.M., Tsyganov S.A.** Shock loading of stratified dusty systems // Archivum Combust. 1989. Vol. 9. No. 1/4. P. 153-165.
3. **Kuhl A.L. et al.** Simulation of a turbulent boundary layer behind a shock // Current Topics in Shock Waves: Proc. 17-th Intern. Symp. on Shock Waves and Shock Tubes / Ed. Kim. AIP Conf. Roc. 1990. P. 762-769.
4. **Kuhl A.L. et al.** Dust scouring by a turbulent boundary layer behind a shock // Archivum Combust. 1989. Vol. 9, No. 1/4. P. 139-147.
5. **Sakakita H., Hayashi A.K. and Ivandaev A.I.** Numerical simulation of shock wave interaction with powder layers Shock Waves / Ed. K.Takayama. Proc. 18-th Intern. Symp. on Shock Waves, Japan 21-26 July, 1991. Heidelberg et al.: Springer-Verlag, 1992. P. 563-568.
6. **Nigmatulin R.I.** Dynamics of multiphase media. Moscow: Nauka, 1974, P. 1-464.
7. **Borisov A.V., Fedorova N.N.** Numerical simulation of turbulent flows near the forward-facing steps // Thermophysics and Aeromechanics. 1996. Vol. 4, No. 1. P. 69-83.
8. **Yabe T.** An universal solver for hyperbolic equations for cubic-polinomial interpolation I. One-dimensional solver // Computer Physics Communication. 1991. Vol. 66. P. 219-232.